



POLİTEKNİK DERGİSİ

*JOURNAL of POLYTECHNIC*

ISSN: 1302-0900 (PRINT), ISSN: 2147-9429 (ONLINE)

URL: <http://dergipark.org.tr/politeknik>



# Numerical and statistical investigation of the effect of composite layer thickness on low-velocity impact behaviour in fibre metal laminate materials

*Fiber metal laminat malzemelerde kompozit katman kalınlığının düşük hızda darbe davranışına etkisinin sayısal ve istatistiksel olarak incelenmesi*

*Yazar(lar) (Author(s)):* Mustafa DÜNDAR<sup>1</sup>, İlyas UYGUR<sup>2</sup>, Ergün EKİCİ<sup>3</sup>, Cihat TAŞÇIOĞLU<sup>4</sup>, Behçet GÜLENCİ<sup>5</sup>

ORCID<sup>1</sup>: 0000-0002-3956-8088

ORCID<sup>2</sup>: 0000-0002-8744-5082

ORCID<sup>3</sup>: 0000-0002-5217-872X

ORCID<sup>4</sup>: 0000-0002-6770-8308

ORCID<sup>5</sup>: 0000-0001-8434-8183

**To cite to this article:** Dündar M., Uygur İ., Ekici E., Taşçıoğlu C. ve Gülenç B., “Numerical and Statistical Investigation of The Effect of Composite Layer Thickness on Low-Velocity Impact Behaviour in Fibre Metal Laminate Materials”, *Journal of Polytechnic*, 29(1):290115:1-8 (2026).

**Bu makaleye şu şekilde atıfta bulunabilirsiniz:** Dündar M., Uygur İ., Ekici E. Taşçıoğlu C., ve Gülenç B., “Numerical and Statistical Investigation of The Effect of Composite Layer Thickness on Low-Velocity Impact Behaviour in Fibre Metal Laminate Materials”, *Journal of Polytechnic*, 29(1):290115:1-8 (2026).

**Erişim linki (To link to this article):** <http://dergipark.org.tr/politeknik/archive>

**DOI:** 10.2339/politeknik.1607678

# Numerical and Statistical Investigation of The Effect of Composite Layer Thickness on Low-Velocity Impact Behaviour in Fibre Metal Laminate Materials

## Highlights

- ❖ Effect of composite layer thickness on the impact behavior of FML materials
- ❖ Effect of striker diameter on peak load, maximum displacement, and absorbed energy
- ❖ Evaluation of parameter effects using statistical methods

## Graphical Abstract

In the study, it was observed that different striker tips and different energy loads were effective on the maximum peak load.

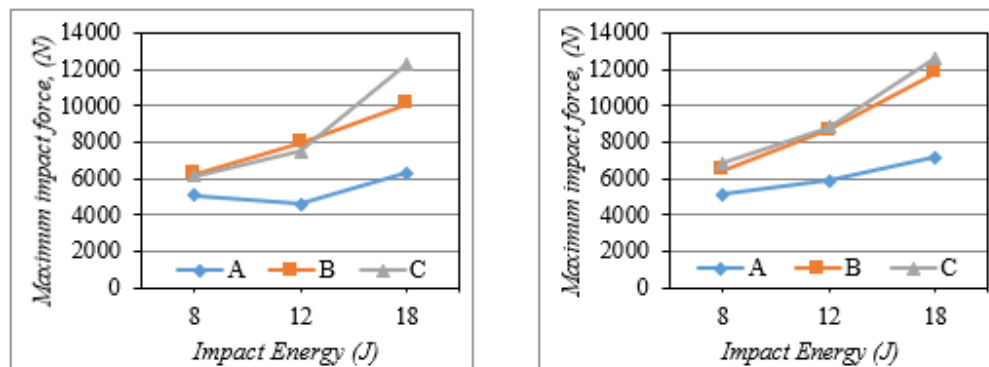


**Figure.** Maximum peak load obtained at different energy loads and different impactor diameters

## Aim

The effects of different composite layer thicknesses and different striker shapes on fibre metal laminate materials were investigated

## Design & Methodology

The mechanical properties of the metal layer used in fibre metal laminate materials were obtained experimentally, while the composite layer was obtained from the finite element program.

## Originality

The issue has not been addressed statistically in the literature

## Findings

Energy load is more effective than other parameters

## Conclusion

The increase in the thickness of the composite layer contributed positively to the values analysed

## Declaration of Ethical Standards

The author(s) of this article declare that the materials and methods used in this study do not require ethical committee permission and/or legal-special permission.

# Numerical and Statistical Investigation of The Effect of Composite Layer Thickness on Low-Velocity Impact Behaviour in Fibre Metal Laminate Materials

(This study was presented at ICMATSE 2024 conference. / Bu çalışma ICMATSE 2247 konferansında sunulmuştur.)

## Research Article / Araştırma Makalesi

Mustafa DÜNDAR<sup>1\*</sup>, İlyas UYGUR<sup>2</sup>, Ergün EKİCİ<sup>3</sup>, Cihat TAŞÇIOĞLU<sup>4</sup>, Behçet GÜLENCİ<sup>5</sup>

<sup>1</sup>Department of Machinery and Metal Technologies, Biga Vocational School, Çanakkale Onsekiz Mart University, Çanakkale, Turkey

<sup>2</sup>Faculty of Engineering, Department of Mechanical Engineering, Düzce University, Duzce, Turkey

<sup>3</sup>Faculty of Engineering, Department of Industrial Engineering, Çanakkale Onsekiz Mart University, Çanakkale, Turkey

<sup>4</sup>Faculty of Forestry, Department of Forest Products Engineering, Düzce University, Duzce, Turkey

<sup>5</sup>Faculty of Technology, Department of Metallurgical and Materials Engineering, Gazi University, Ankara, Turkey

(Geliş/Received : 26.12.2024 ; Kabul/Accepted : 10. 05.2025; Erken Görünüm/Early View : 22.05.2025)

## ABSTRACT

In the field of aviation, reducing fuel costs by designing lighter vehicles and thus producing more environmentally friendly aircraft is one of the most important issues. This situation has led aircraft manufacturers to search for lighter and more durable materials. For this reason, Fibre Metal Laminate (FML) structures, which are used especially in the aerospace industry due to their superior fatigue and impact resistance properties, attract attention. Carbon fibre reinforced aluminium plates (CARALL), the most unique member of the FML hybrid structure family, has attracted the attention of researchers. In this study, the low-velocity impact behaviour of CARALL FML structures with different composite layer thicknesses at different energy loading (8J-12J-18J) and different impactor types (Ø15 and Ø20) were statistically investigated. CARALL FML structures were modelled in 2/1 arrangement (Al-0°<sub>[1]</sub>-Al, Al-0°<sub>[3]</sub>-Al, Al-0°<sub>[5]</sub>-Al) in LS-DYNA finite element programme. It is observed that the peak load Fmax increases with increasing energy loading. The increase in striker diameter decreased the amount of absorbed energy and increased the rebound.

**Keywords:** Fiber Metal Laminat, Low-velocity impact, composite, CFRP, FML, Numerical Analysis, CARALL, ANOVA.

## Fiber Metal Laminat Malzemelerde Kompozit Katman Kalınlığının Düşük Hızda Darbe Davranışına Etkisinin Sayısal ve İstatistiksel Olarak İncelenmesi

### ÖZ

Havacılık alanında daha hafif araç tasarlayarak yakıt maliyetleri düşürmek böylelikle daha çevreci hava araçları üretmek en önemli konuların başında gelmektedir. Bu durum uçak üretici firmaların daha hafif ve dayanıklı malzeme arayışına yöneltmiştir. Bu sebepten dolayı özellikle havacılık endüstrisinde üstün yorulma ve darbe dayanımı özelliklerinden dolayı kullanılan Fiber Metal Laminat(FML) yapılar ilgi çekmektedir. FML hibrit yapı ailesinin en özgün üyesi olan karbon elyaf takviyeli alüminyum plakalara(CARALL) araştırmacıların ilgisini çekmektedir. Bu çalışmada farklı kompozit katman kalınlığına sahip CARALL FML yapıların farklı enerji yüklemesi(8J-12J-18J) ve farklı vurucu tiplerinde(Ø15 ve Ø20) düşük hızda darbe davranışı istatistiksel olarak incelenmiştir. CARALL FML yapılar 2/1 dizilimde (Al-0°<sub>[1]</sub>-Al, Al-0°<sub>[3]</sub>-Al, Al-0°<sub>[5]</sub>-Al) olacak şekilde LS-DYNA sonlu elemanlar programında modellenmiştir. Enerji yüklemesinin artmasıyla beraber Fmax tepe yükünün arttığı gözlemlenmiştir. Vurucu çapının artması absorbe edilen enerji miktarını düşürürken geri tepmeyi artırmıştır.

**Anahtar Kelimeler:** Fiber Metal Laminat, Düşük hızda darbe, composite, CFRP, FML, Sayısal Analiz, CARALL, ANOVA.

### 1. INTRODUCTION

Composite material is a new generation material type designed to improve the disadvantageous properties of the main group materials. They are generally preferred because they are lightweight, many mechanical, physical and technological properties can be modified and optimized, and they are relatively economic. They are

used especially in home and sporting goods, aviation and transportation industries. Compared to classical types and alloys, there are material groups with very important advantages, metal, ceramic and polymer based types. Their tensile, hardness, impact, fatigue properties are quite good [1]–[8].

\*Sorumlu Yazar (Corresponding Author)  
e-posta : m.dundar@comu.edu.tr

Fibre Metal Laminate materials (FMLs) are new types of composites hybrid structures formed by combining thin metal layers with composite layers [9], [10]. The most remarkable feature of FML materials is to combine the light weight of fibre reinforced polymer (FRP) materials with the good impact resistance of the metal layer [11]. FML materials were first developed in 1978 [12]. In the meantime, only Aramid fibre reinforced aluminium laminate and glass fibre reinforced aluminium laminate (GLARE) product models have matured and started to be used in the aerospace industry. However, with the development of technology in the following years, carbon fibre reinforced aluminium laminates started to attract attention [13]. Carbon fibre reinforced composites have a large area of use due to their performance and light weight [14]. Due to these superior properties, studies have focused on CARALL FML materials. CARALL materials provide great advantages for the aerospace industry [15].

FML materials are mostly used in the aerospace industry. According to statistics, more than 13% of aviation accidents are caused by impact damage [16]. Impact damage can occur at high and low-velocity. Impacts occurring at high velocity can be visually recognized and intervened. However, unlike high velocity, low-velocity impact can cause damage that is not visible to the eye [17]. Low velocity impact is usually dominated by in-plane stresses. This leads to the formation of different damage modes in the internal structure of the structure. It is impossible to determine this intuitively. This situation jeopardises the safety of the structure [18]. For these reasons, low velocity impact damage is one of the important damage conditions in FML materials. Therefore, it is an issue that needs to be investigated in detail at different energy loads and different impact properties of the structure to guide the design and development of the next generation CARALL FML materials. In their study, Sharma et al. [19] produced FML materials in 2/1, two different 3/2 and 4/3 formats by keeping the aluminium layer thickness constant. In the experiments, they observed that increasing the thickness of the structure decreases the degree of damage and increases the maximum peak load. Yaghoubi et al. [20] investigated the impact behaviour of 5 different GLARE types such as 2/1, 3/2, 4/3, 5/4 and 6/5. They reported that the critical behaviour of fibre and aluminium depends on the thickness of the panel. They stated that the threshold cracking energy varies parabolically with the thickness of the specimen. Lalibert et al. [21] investigated the anti-impact properties of three different types of FML, each with different layers. They reported that the specimen with higher fibre content absorbed less energy and was subjected to lower damage. Fan et al. [22] observed that increasing both the number of metal layers and the thickness of the composite layer increased the puncture resistance. Ataş [23] investigated the damage mechanisms of GLARE materials. They determined that fibre fracture and delamination in the layers are the primary energy absorbing mechanisms. Sadighi et al.

[24] observed that increasing the thickness of the metal layer increases the impact resistance. It has been proved that the contact shape between the impactor and the structure has a significant effect on the impact response of general structures [25], [26]. De Cicco et al. [27] investigated the low velocity impact behavior of magnesium FMLs under impact forces of different sizes and shapes. According to the experimental results, while cracks and delamination occurred in the metal layers in the tests performed with the sharp-edged impact tip, it was observed that the hemispherical tips had a greater effect on residual deformation. Yao et al. [28] investigated the low velocity impact behavior of FML materials under various impactor shapes and energy loads. At the end of the study, they stated that the impact behavior of FMLs strongly depends on the striker shape, energy load and metal layer distribution.

In this study, we applied different composite layer thickness (0.5 mm) of different composite layer thickness (Al-0°<sub>[1]</sub>-Al, Al-0°<sub>[3]</sub>-Al, Al-0°<sub>[5]</sub>-Al), The effect of different striker shapes (Ø15-Ø20) and different energy loads (8J-12J-18J) on the impact behaviour at low-velocity was investigated numerically and statistically.

## 2. MATERIAL and METHOD

FML structures are materials that are formed by the combination of metal and composite structure. In this study, Al2024-T3 material with a thickness of 0.5 mm obtained from AMAG Rolling company was preferred as the metal layer. Detailed research has been conducted for 2xxx series of Al-alloy composites [1]–[8]. Tensile test specimens were prepared in accordance with TS EN ISO 6892-1 standards in order to use engineering data in numerical analysis of Al2024-T3 material used in the study. The prepared tensile test specimens were carried out on a Zwick/Roell Z600 tensile testing machine (Figure 1.). The tensile test data of Al2024-T3 material obtained as a result of the tensile test were added to the LS\_DYNA related material card.

### 2.1. Multilayer Design

The CARALL structure was modelled in 2/1 format to consist of 3 layers. The top and bottom plates consist of Al2024-T3 material, while the middle layer has a CFRP structure. All CARALL materials are in 2/1 format and modelled in LS\_DYNA program in such a way that only the composite layer thickness increases. The layer arrangement is shown in table 1 and figure 2. In all materials, the metal layer thickness is 1 mm in two layers. Each layer thickness of CFRP layers is 0.4 mm. Fibre orientations are modelled as 0° for all material groups. CARALL materials were modelled as multilayer shell elements with 3 different material codes. Material identification was made for each layer. The test specimens were designed as Ø40 mm diameter. Experiments were carried out with Ø20 and Ø15 mm striking tips with 8J, 12J and 18J values.

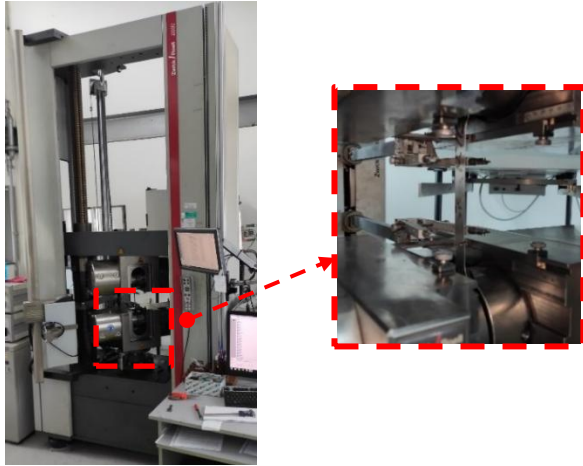
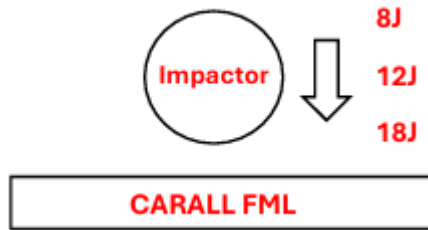


Figure 1. Tensile test of Al2024-T3 material

**Table 1. Configuration of CARALL plates**

Material Code	Lay-up	Total Thickness
A	Al-0° <sub>[1]</sub> -Al	1.4 mm
B	Al-0° <sub>[3]</sub> -Al	2.2 mm
C	Al-0° <sub>[5]</sub> -Al	3 mm



a) Schematic representation

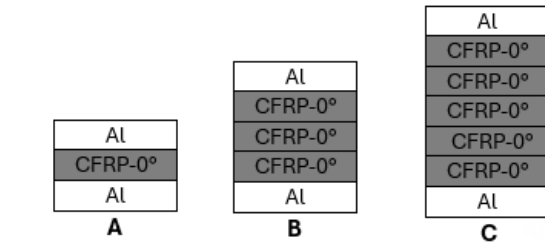
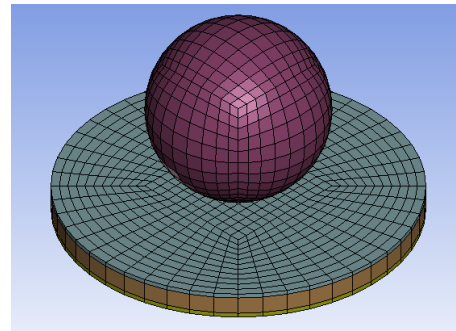


Figure 2. Stacking sequence of CARALL materials

CARALL material The top and bottom plates consist of 0.5 m thick Al2024-T3 plates. In the middle layer there is a CFRP composite structure as shown in Table 1. All FML materials are stacked in 2/1 format. FML materials are modelled as shell elements in multiple layers. Material identification was made for each layer. Test specimens were designed in Ø40 mm diameter. Experiments were carried out with Ø20 and Ø15 striking tips with 8J, 12J and 18J values (Figure 3).



b) Experimental setup

Figure 3. Schematic representation and experimental setup of the low- velocity impact test

The Johnson-Cook material model was used to utilize the properties of the Al2024-T3 material used in the CARALL material. The Johnson-Cook material model best describes high strain rates and large deformation rates. It is widely used in researches due to its simplicity [29]. Johnson-Cook material model shows linear behaviour below the yield limit and plastic behaviour above the yield limit. The strain equation between stress and strain unit is shown in equation 1.

$$\sigma = [A + B\epsilon^n] \left[ 1 + C \ln \frac{\dot{\epsilon}}{\dot{\epsilon}_0} \right] [1 - [T^*]^m] \quad (1)$$

Where;  $\sigma$  is yield strength,  $A$  is yield stress,  $B$  is modulus of consolidation,  $\epsilon$  is plastic strain,  $n$  is plastic strain exponent,  $C$  is strain constant,  $\dot{\epsilon}$  is deformation rate,  $\dot{\epsilon}_0$  is reference deformation rate,  $m$  is temperature exponent and  $T^*$  is melting temperature in Kelvin.

In the case of stresses exceeding the yield limit, rupture will start as soon as the maximum plastic elongation value (rupture limit) is exceeded. Johnson-Cook damage criterion is given in equation (2).

$$\epsilon_f = \left[ D_1 + D_2 + \exp \left( D_3 \frac{\sigma_m}{\sigma_s} \right) \right] \left[ 1 + D_4 \ln \frac{\dot{\epsilon}}{\dot{\epsilon}_0} \right] [1 + D_5 T^*] \quad (2)$$

Where;  $D_1, D_2, D_3, D_4, D_5$  are damage parameters,  $\sigma_m$  is the average of normal stresses in three directions,  $\sigma_s$  is the von Mises equivalent stress. The experimentally obtained mechanical properties of Al2024-T3 material as described in section 2 are shown in table 2.

Table 2. Mechanical properties of Al2024-T3 material

Mechanical properties	Units	Value
Elastic Modulus	E (GPa)	72
Poisson Ratio	$\nu$	0.33
Yield Strength	$\sigma_{\%0.2}$ (MPa)	358

The MAT054-055 material card is an improved version of the Chang-Chang composite damage model. This model is used for thin shells. The model is assumed to be elastic in the absence of damage. But when damage occurs, it is assumed to be nonlinear. MAT022 is an

improved version of the material card. In the context of material formulation, Chang/Chang (MAT-54) can be calculated by means of the following equations:

#### Tensile Fibre Mode

$$\sigma_{aa} > 0 \rightarrow e_f = \left(\frac{\sigma_{aa}}{X_t}\right) + \beta \left(\frac{\sigma_{ab}}{S_c}\right)^2 - 1 \begin{cases} \geq 0 & \text{Failed} \\ < 0 & \text{Elastic} \end{cases} \quad (3)$$

$$E_a = E_b = G_{ab} = \nu_{ba} = \nu_a = 0$$

#### Compression Fibre Mode

$$\sigma_{aa} < 0 \rightarrow e_c^2 = \left(\frac{\sigma_{aa}}{X_c}\right)^2 - 1 \begin{cases} \geq 0 & \text{Failed} \\ < 0 & \text{Elastic} \end{cases} \quad (4)$$

$$E_a = \nu_{ba} = \nu_{ab} = 0$$

#### Tensile Matrix mode

$$\sigma_{bb} > 0 \rightarrow e_m^2 = \left(\frac{\sigma_{bb}}{Y_t}\right) + \beta \left(\frac{\sigma_{ab}}{S_c}\right)^2 - 1 \begin{cases} \geq 0 & \text{Failed} \\ < 0 & \text{Elastic} \end{cases} \quad (5)$$

$$E_b = \nu_{ba} = 0. \rightarrow G_{ab} = 0$$

#### Compression Matrix Mode

$$\sigma_{bb} < 0 \rightarrow e_d^2 = \left(\frac{\sigma_{bb}}{Y_c}\right)^2 + \left[\left(\frac{\sigma_{ab}}{S_c}\right)^2 - 1\right] \left(\frac{\sigma_{bb}}{Y_c}\right) + \left(\frac{\sigma_{ab}}{S_c}\right)^2 - 1 \begin{cases} \geq 0 & \text{Failed} \\ < 0 & \text{Elastic} \end{cases} \quad (6)$$

$$E_b = \nu_{ba} = \nu_{ab} = 0. \rightarrow G_{ab} = 0$$

$$X_c = 2Y_c, \%50 \text{ for fiber volume}$$

The mechanical properties of the CFRP structure used in the composite layer were taken from the ANSYS material library. These constants were integrated into the MAT054-055 material card in Ls-Dyna. The engineering constants of the CFRP materials used are shared in Table 3.

**Table 3.** Mechanical Properties of CFRP Materials

Mechanical properties	Symbols and Units	Value
Density	gr/cm <sup>3</sup>	1.54
1 direction Elasticity Modulus	$E_1$ (GPa)	123
2 direction Elasticity Modulus	$E_2$ (GPa)	9.87
Poisson Ratio	$\nu_{12}$	0.27
1 direction tensile strength	$X_T$ (MPa)	1979
1 direction tensile strength	$Y_T$ (MPa)	26
1 direction compersion strength	$X_C$ (MPa)	893
2 direction compersion strength	$Y_C$ (MPa)	139
Shear strength	$S_C$ (MPa)	100

The CONTACT\_ONE\_WAY\_SURFACE\_TO\_SURFACE TIEBREAK card is used to define the

aluminium/composite interface. This card connects the nodes that are initially in contact until a certain criterion is met as follows.

$$\left(\frac{|\sigma_n|}{NFLS}\right)^2 + \left(\frac{|\sigma_s|}{SFLS}\right)^2 \geq 1 \quad (7)$$

NFLS and SFLS are the interfacial normal and shear strengths, respectively. In this study, the interlaminar shear and normal strengths for the aluminium/composite interface were chosen as 80 MPa and 40 MPa, respectively.

In this experimental setup, it is assumed that the striker is not damaged and modelled rigidly using MAT020 board. The material properties of the striking tip using MAT20 are defined in Table 4.

**Table 4.** MAT20 steel material properties [30]

Mechanical properties	Symbols and Units	Value
Elastic Modulus	E (GPa)	210
Poisson Ratio	$\nu$	0.33
Density	gr/cm <sup>3</sup>	7.8

### 3. RESULTS AND DISCUSSION

The maximum peak load ( $F_{max}$ ) is defined as the resistance of the specimen to the impact load in the low-velocity test [31]. A high peak load means that the resistance of the material against impact is high. When the graphs of the maximum peak load in Figure 4 are examined, the increase in the thickness of the composite layer led to an increase in the maximum peak load in all energy loads (8J-12J-18J) and in all samples. This situation shows that the increase in thickness is an effective factor in the load carrying capacity of the material. It shows that in specimens with low thickness, many damage modes occur in specimens where the peak load does not increase according to the energy load and the bearing capacity is lost [32]. It is seen in the figures that the striker diameter is another factor in peak loads. This shows that the contact area between the CARALL material and the striker is an important factor and is effective in the maximum peak load. It was found that as the contact area increases, the peak load increases [33].

The maximum displacement is the displacement of the specimen and the impactor which is damaged during impact. When Figure 5 is analysed, it is seen that the maximum displacement decreases with the increase in the diameter of the striker. This is related to the contact area between the impactor and the specimen. As the contact area decreases, as a result of the application of the applied energy load to a smaller area, the formation of more damage modes caused more displacement in the material [34]. In addition, since the amount of energy per unit area increases, the increase in the amount of damage is the main factor. In all specimens, the maximum displacement increased as the energy load increased. However, the increase in material thickness decreased the displacement.

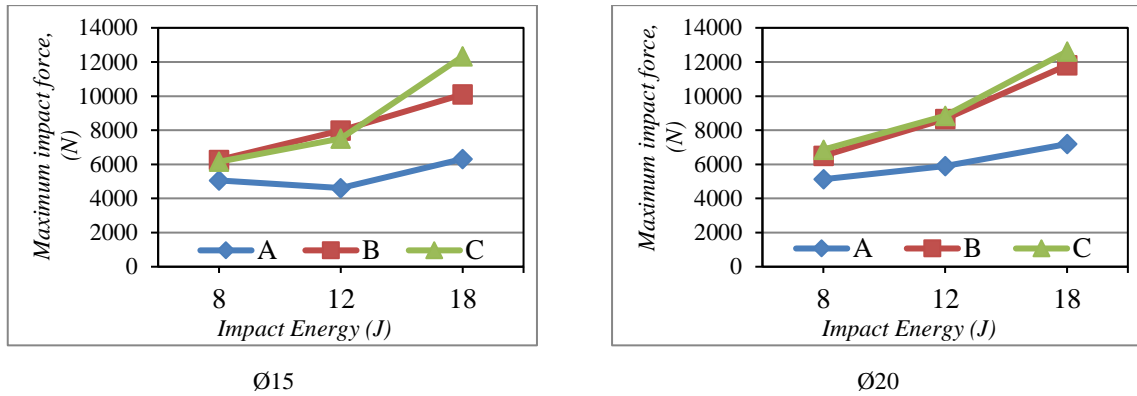


Figure 4. Maximum peak load obtained at different energy loads and different impactor diameters

As the energy capacity per unit area increases, the displacement decreases. Therefore, as the material thickness increases, the energy is spread over a larger

volume and the energy per unit area decreases, thus the displacement also decreases. It is seen that energy load is the main factor in displacement in all specimens.

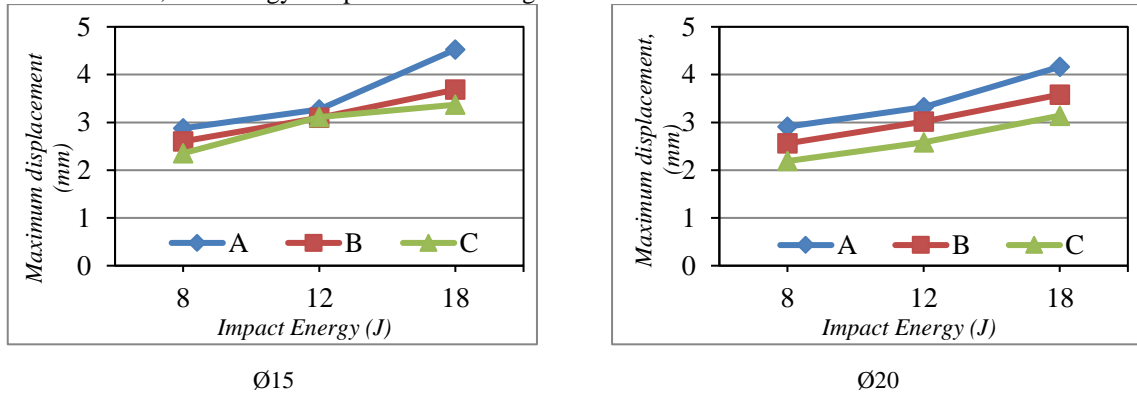


Figure 5. Maximum displacement obtained at different energy loads and different impactor diameters

The graphs of the absorbed energy amounts obtained at different energy loads are shown in Figure 6. In all experiments and all specimens, the best result was obtained in C coded specimen. Increasing the thickness of the composite layer decreased the amount of absorbed energy. This shows that the material utilises more energy by recoil. The decrease in the diameter of the impactor increased the amount of absorbed energy. The decrease in the contact area indicates that more damage

mechanisms occur due to the effect of more energy on that area [35]. The increase in the amount of absorbed energy indicates that the energy absorption capacity per unit decreases in the samples [28]. Increasing the impactor diameter and increasing the composite layer thickness decreased the absorbed energy. It was observed that the most effective factor in all specimens was impact energy.

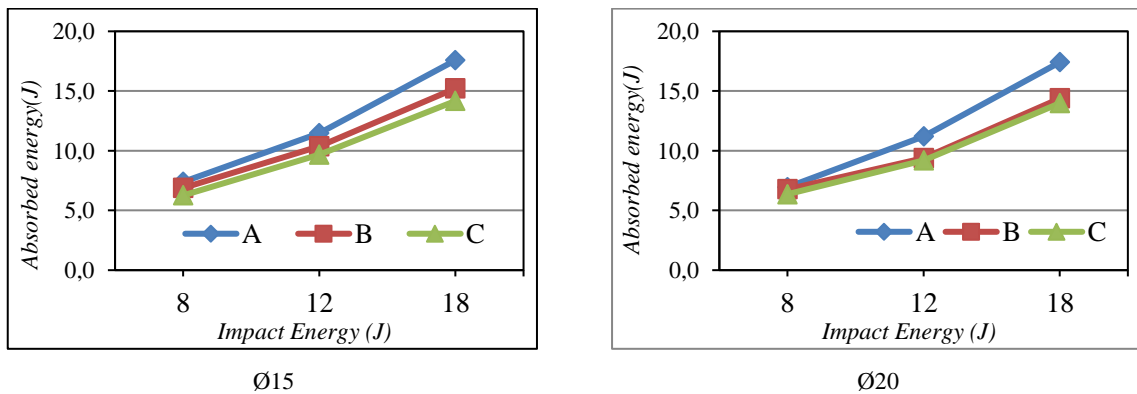


Figure 6. Absorbed energy obtained at different energy loads and different impact diameters

### 3.1. Variance Analysis (ANOVA)

Analysis of variance (ANOVA) was applied at 95% confidence level to determine parameter effects and effect levels. The results of ANOVA at 95% confidence level for all response variables are presented in Table 5. In terms of P values for the amount of absorbed energy, it is seen that the interaction of material, striker diameter, impact energy and material\*impact energy (M\*DE) is significant at  $P < 0.05$  and impact energy is the most effective parameter with a contribution rate of 92.44%. It was followed by material and M\*DE interaction with 5.44% and 1.64% contribution rates, respectively. All other factors and factor interactions had no significant contribution ( $< 1\%$ ).

### 4. CONCLUSION

1. Increasing the composite thickness increased the maximum peak load.

2. Increasing the composite thickness decreased the amount of absorbed energy and maximum displacement.
3. Reducing the diameter of the striker caused different damage mechanisms due to the lower contact area. This had a negative effect on all variables.
4. According to the ANOVA results; it was seen that impact energy was the most effective parameter with 92.442% contribution rate for the amount of absorbed energy, material and impact energy for maximum peak load with 37.161% and 49.202% contribution rates respectively, impact energy for maximum displacement with 66.38% contribution rate.

**Table 5.** ANOVA results for all response variables

Amount of energy absorbed						
<i>F</i>	<i>SD</i>	<i>KT</i>	<i>KO</i>	<i>F-Value</i>	<i>P- Value</i>	<i>KO (%)</i>
Ç	1	0.644	0.644	13.7	0.021*	0.259
M	2	13.542	6.771	143.95	0*	5.449
DE	2	229.756	114.878	2442.35	0*	92.442
Ç*M	2	0.174	0.087	1.85	0.27	0.070
Ç*DE	2	0.141	0.07	1.49	0.328	0.057
M*DE	4	4.096	1.024	21.77	0.006*	1.648
Error	4	0.188	0.047			0.076
Total	17		248.541			100
$R^2 = \%99.92, R^2_{(Adjusted\ for)} = \%99.68$						
Maximum peak load, Fmax						
Ç	1	2858441	2858441	15.26	0.017*	2.708
M	2	39227079	19613540	104.7	0*	37.161
DE	2	51937373	25968687	138.63	0*	49.202
Ç*M	2	12249	6125	0.03	0.968	0.012
Ç*DE	2	489226	244613	1.31	0.366	0.463
M*DE	4	10285184	2571296	13.73	0.013*	9.744
Error	4	749321	187330			0.710
Total	17		105558874			100
$R^2 = \%99.29, R^2_{(Adjusted\ for)} = \%96.98$						
Maximum displacement						
Ç	1	0.11392	0.11392	6.64	0.062	1.849
M	2	1.57216	0.78608	45.8	0.002*	25.523
DE	2	4.08882	2.04441	119.12	0*	66.380
Ç*M	2	0.05014	0.02507	1.46	0.334	0.814
Ç*DE	2	0.02463	0.01231	0.72	0.542	0.400
M*DE	4	0.24135	0.06034	3.52	0.125	3.918

**Table 5. (Cont.)** ANOVA results for all response variables

Error	4	0.06865	0.01716	1.115
Total	17	6.15968		100

$R^2=98.89\%$ ,  $R^2_{(Adjusted\ for)}=95.26\%$

Abbreviations: C; Impactor diameter, M; Material, DE; Impact energy, F; Factors, SD; Degrees of freedom, SD; Sum of squares, KO; Mean of squares, %CR; Contribution rate

\*\* indicates significant terms with  $P<0.05$ .

**DECLARATION OF ETHICAL STANDARDS**

The author(s) of this manuscript declare that the materials and methods used in their studies do not require ethics committee approval and/or legal-specific permission

**AUTHORS’ CONTRIBUTIONS**

**Mustafa DÜNDAR:** Proposed the main idea of the study, conducted numerical analyses, evaluated the data, and prepared the initial draft of the manuscript.

**İlyas UYGUR:** Provided guidance in method development, experimental design, and numerical modelling; ensured the scientific integrity of the study and contributed to the final version of the manuscript.

**Ergün EKİCİ:** Performed finite element modelling using LS-DYNA software and contributed to the preparation of material definitions and analysis cards.

**Cihat TAŞCIOĞLU:** Conducted mechanical tests, collected experimental data, and participated in the setup of the experimental apparatus.

**Behçet GÜLENC:** Supervised the project, provided scientific oversight, and contributed editorially to the final version of the manuscript.

**CONFLICT OF INTEREST**

There is no conflict of interest in this study.

**REFERENCES**

[1] Uygur I., “Notch behavior and fatigue life predictions of discontinuously reinforced MMCs”, *Archives of Metallurgy and Materials*, 56(1): 109–115, (2011).

[2] Uygur I., “Tensile Behavior Of Powder Metallurgy Processed (Al-Cu-Mg-Mn) /SiCp Composites”, *Iranian Journal of Science & Technology*, 28(B2): 239–248, (2004).

[3] Uygur I., “Comparison of fatigue crack growth rates for particulate reinforcement composite and base alloy”, in *Properties of Materials*, I. Uygur (Ed.), Bidge Pub, 77–87, (2023).

[4] Uygur I., Gulenç B., “The effect of shielding gas composition for MIG welding process on mechanical behaviour of low carbon steel”, *Metallurgija*, 43(1): 35–40, (2004).

[5] Uygur I., Evans W., Bache M., Gulenç B., “The fatigue behaviour of aluminium alloy 2124 reinforced with SiC

particulates”, *Metallofizyka i Novejshe Tekhnologii*, 26(7): 927–939, (2004).

[6] Uygur I., Dogan I., “The effect of TIG welding on microstructure and mechanical properties of a butt-jointed-unalloyed titanium”, *Metallurgija*, 44(2): 119–123, (2005).

[7] Uygur I., Cicek A., Toklu E., Kara R., Saridemir S., “Fatigue life predictions of metal matrix composites using artificial neural networks”, *Archives of Metallurgy and Materials*, 59(1): 97–103, (2014).

[8] Uygur I., “Influence of Particle Sizes and Volume Fractions on Fatigue Crack Growth Rates of Aerospace Al-Alloys Composites”, *Archives of Metallurgy and Materials*, 69(1): 337–341, (2024).

[9] Pang Y., Yan X., Yao H., Qu J., Wu L., “Experimental study of basalt fiber/steel hybrid laminates under low-velocity impact”, *Engineering Fracture Mechanics*, 259: 108169, (2022).

[10] Bienias J., Jakubczak P., Dadej K., “Low-velocity impact resistance of aluminium glass laminates – Experimental and numerical investigation”, *Composite Structures*, 152: 339–348, (2016).

[11] Hou W., Li M., Zhang X., Liu Z., Sang L., “Design and optimization of the bumper beam with corrugated core structure of fiber metal laminate subjected to low-velocity impact”, *Thin-Walled Structures*, 187: 110746, (2023).

[12] Sinmazçelik T., Avcu E., Bora M.Ö., Çoban O., “A review: Fibre metal laminates, background, bonding types and applied test methods”, *Materials and Design*, 32(7): 3671–3685, (2011).

[13] Lu B., Zhang J., Zheng D., Xie J., Zhang L., “Theoretical analysis on carbon fiber reinforced aluminum laminate under off-center impact”, *International Journal of Mechanical Sciences*, 248: 108247, (2023).

[14] Hynes N.R.J., Vignesh N.J., Jappes J.T.W., Velu P.S., Barile C., Ali M.A., Farooq M.U., Pruncu C.I., “Effect of stacking sequence of fibre metal laminates with carbon fibre reinforced composites on mechanical attributes: Numerical simulations and experimental validation”, *Composites Science and Technology*, 221: 109303, (2022).

[15] Song S.H., Byun Y.S., Ku T.W., Song W.J., Kim J., Kang B.S., “Experimental and Numerical Investigation on Impact Performance of Carbon Reinforced Aluminum Laminates”, *Journal of Materials Science & Technology*, 26(4): 327–332, (2010).

[16] Wei S., Zhang X., Li Y., Wang T., Huang Q., Liu C., Guan H., “Study of the dynamic response and damage evolution of carbon fiber/ultra-thin stainless-steel strip fiber metal laminates under low-velocity impact”, *Composite Structures*, 330: 117772, (2024).

- [17] Chai G.B., Manikandan P., “Low velocity impact response of fibre-metal laminates – A review”, *Composite Structures*, 107: 363–381, (2014).
- [18] Xin H., Tao J., Xiaomin M., Xuefeng S., Xin L., “Dynamic response of single curved fiber-metal hybrid lamina composites subject to low-velocity impact”, *International Journal of Impact Engineering*, 164: 104209, (2022).
- [19] Sharma A.P., Khan S.H., Kitey R., Parameswaran V., “Effect of through thickness metal layer distribution on the low velocity impact response of fiber metal laminates”, *Polymer Testing*, 65: 301–312, (2018).
- [20] Seyed Yaghoubi A., Liu Y., Liaw B., “Low-Velocity Impact on GLARE 5 Fiber-Metal Laminates: Influences of Specimen Thickness and Impactor Mass”, *Journal of Aerospace Engineering*, 25(3): 409–420, (2012).
- [21] Laliberté J.F., Straznicki P.V., Poon C., “Impact Damage in Fiber Metal Laminates, Part 1: Experiment”, *AIAA Journal*, 43(11): 2445–2453, (2005).
- [22] Fan J., Cantwell W.J., Guan Z.W., “The low-velocity impact response of fiber-metal laminates”, *Journal of Reinforced Plastics and Composites*, 30(1): 26–35, (2010).
- [23] Atas C., “An Experimental Investigation on the Impact Response of Fiberglass/Aluminum Composites”, *Journal of Reinforced Plastics and Composites*, 26(14): 1479–1491, (2007).
- [24] Sadighi M., Pärnänen T., Alderliesten R.C., Sayeafabi M., Benedictus R., “Experimental and numerical investigation of metal type and thickness effects on the impact resistance of fiber metal laminates”, *Applied Composite Materials*, 19(3–4): 545–559, (2012).
- [25] Mohagheghian I., McShane G.J., Stronge W.J., “Impact perforation of monolithic polyethylene plates: Projectile nose shape dependence”, *International Journal of Impact Engineering*, 80: 162–176, (2015).
- [26] Ferrante L., Sarasini F., Tirillò J., Lampani L., Valente T., Gaudenzi P., “Low velocity impact response of basalt-aluminium fibre metal laminates”, *Materials & Design*, 98: 98–107, (2016).
- [27] De Cicco D., Asaee Z., Taheri F., “Low-velocity impact damage response of fiberglass/magnesium fiber-metal laminates under different size and shape impactors”, *Mechanics of Advanced Materials and Structures*, 24(7): 545–555, (2017).
- [28] Yao L., Wang C., He W., Lu S., Xie D., “Influence of impactor shape on low-velocity impact behavior of fiber metal laminates combined numerical and experimental approaches”, *Thin-Walled Structures*, 145: 106399, (2019).
- [29] Hallquist J.O., *LS-DYNA® Theory Manual*, (2006).
- [30] Dhaliwal G.S., Newaz G.M., “Modeling Low Velocity Impact Response of Carbon Fiber Reinforced Aluminum Laminates (CARALL)”, *Journal of Dynamic Behavior of Materials*, 2(2): 181–193, (2016).
- [31] Dündar M., Uygur İ., Ekici E., “Optimization of low-velocity impact behavior of FML structures at different environmental temperatures using taguchi method and grey relational analysis”, *Journal of Composite Materials*, 59(7): 885–906, (2025).
- [32] Bienias J., Jakubczak P., “Impact damage growth in carbon fibre aluminium laminates”, *Composite Structures*, 172: 147–154, (2017).
- [33] Sevkat E., Liaw B., Delale F., “Drop-weight impact response of hybrid composites impacted by impactor of various geometries”, *Materials & Design (1980–2015)*, 52: 67–77, (2013).
- [34] Nakatani H., Kosaka T., Osaka K., Sawada Y., “Damage characterization of titanium/GFRP hybrid laminates subjected to low-velocity impact”, *Composites Part A: Applied Science and Manufacturing*, 42(7): 772–781, (2011).
- [35] Fathi A., Liaghat G., Sabouri H., “An experimental investigation on the effect of incorporating graphene nanoplatelets on the low-velocity impact behavior of fiber metal laminates”, *Thin-Walled Structures*, 167: 108162, (2021).